

# Sustainable and Versatile CuO/GNS Nanocatalyst for Highly Efficient Base Free Coupling Reactions

Mayakrishnan Gopiraman,<sup>†</sup> Dian Deng,<sup>†</sup> Sundaram Ganesh Babu,<sup>†</sup> Takuya Hayashi,<sup>‡</sup> Ramasamy Karvembu,<sup>\*,§</sup> and Ick Soo Kim<sup>\*,†</sup>

<sup>†</sup>Nano Fusion Technology Research Lab, Interdisciplinary Cluster for Cutting Edge Research (ICCER), Division of Frontier Fibers, Institute for Fiber Engineering (IFES), National University Corporation, Shinshu University, Ueda, Nagano 386 8567, Japan

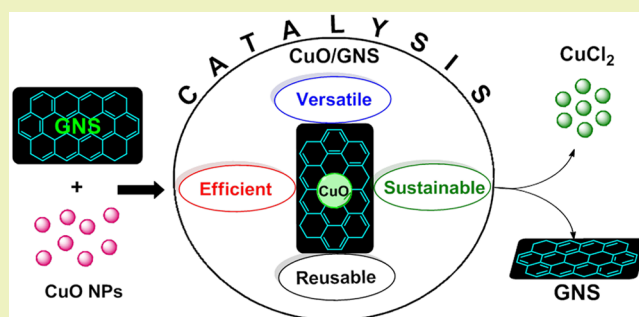
<sup>‡</sup>Faculty of Engineering, Shinshu University, 4-17-1 Wakasato, Nagano 380 8553, Japan

<sup>§</sup>Department of Chemistry, National Institute of Technology, Tiruchirappalli 620 015, India

## S Supporting Information

**ABSTRACT:** A CuO nanoparticles (CuO NPs)/graphene nanosheet (GNS) hybrid was prepared by a very simple method and employed as a nanocatalyst (CuO/GNS) for base free coupling reactions, namely, A<sup>3</sup>-coupling and *aza*-Michael reactions. TEM shows that CuO NPs of below ~35 nm size are homogeneously dispersed on the GNS. Strong adhesion between CuO NPs and GNS was acknowledged by a high Raman I<sub>D</sub>/I<sub>G</sub> ratio and XPS result. The BET surface area of CuO/GNS was found to be 66.26 m<sup>2</sup> g<sup>-1</sup>. The EDS and XPS investigations revealed that the weight percentage and chemical state of Cu in CuO/GNS were 4.46% and +2, respectively. Under mild reaction conditions, CuO/GNS exhibited an outstanding catalytic activity in terms of yield, turnover number (TON) and turnover frequency (TOF) toward A<sup>3</sup>-coupling reaction. A small amount of catalyst (10 mg, 0.7 mol % of Cu) is enough to carry out the reactions with a wide range of substrates. The CuO/GNS is stable, heterogeneous in nature and reusable for at least five times without any significant losses of yield. N-oxidation of tertiary amines was also carried out to explore further the activity of CuO/GNS, and the results are found to be excellent. Versatility of the CuO/GNS was realized from the superior catalytic activity of used CuO/GNS in *aza*-Michael reaction. Finally, GNS (~95%) and CuO (as CuCl<sub>2</sub>) were successfully recovered from the used CuO/GNS and confirmed by TEM, Raman, XPS, XRD and SEM-EDS analyses.

**KEYWORDS:** Graphene nanosheets, Copper oxide, Coupling reactions, Reusable, Versatile, Sustainable



## INTRODUCTION

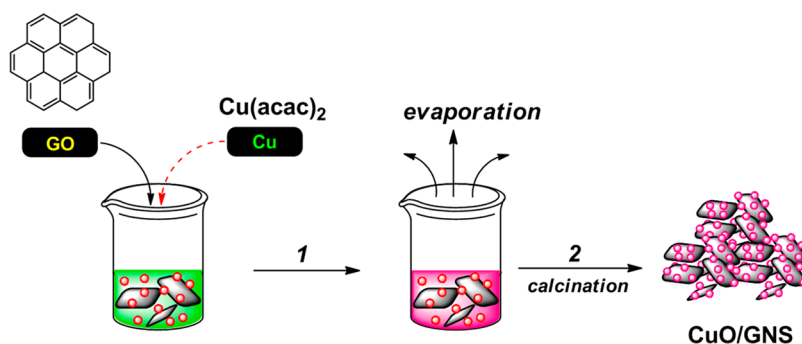
Propargylamines have played a tremendous role as precursors/intermediates in the construction of interesting organic building blocks such as biologically active compounds, highly valuable drugs, natural products and nitrogen-containing heterocycles.<sup>1,2</sup> Some propargylamine derivatives are used as essential neuroprotective and antiapoptotic agents.<sup>3</sup> There are some conventional synthetic methodologies for propargylamines, but they are limited due to the use of stoichiometric amounts of moisture sensitive organometallic reagents.<sup>4,5</sup> Recently, multi-component reactions (MCRs) have received much attention due to their simple procedure, synthetic efficiency, high selectivity and intrinsic atom economy.<sup>6</sup> Particularly, three-component coupling of aldehyde, alkyne and amine, known as A<sup>3</sup>-coupling, is a prime route and a widely used tool to synthesize propargylamines and their derivatives.<sup>7,8</sup> Organogold complexes,<sup>9</sup> Au-salts,<sup>10</sup> Hg<sub>2</sub>Cl<sub>2</sub><sup>11</sup> and Ag-salts,<sup>12</sup> are the most common homogeneous catalysts for the A<sup>3</sup>-coupling reaction. Because of easy preparation and exceptional physicochemical properties such as high stability, reusability and easy recovery,

transition metals-based heterogeneous catalysts are often preferred.<sup>13</sup> Nevertheless, until now, most of the reported A<sup>3</sup>-coupling reactions are performed by using either expensive metal catalysts or stoichiometric quantities of organometallic reagents.<sup>14</sup> Zhang et al.<sup>15</sup> prepared metal oxide supported Au(III) catalysts for three-component coupling reactions. Reddy and co-workers<sup>16</sup> used silver salt of 12-tungstophosphoric acid (Ag<sub>3</sub>PW<sub>12</sub>O<sub>40</sub>) to catalyze the A<sup>3</sup>-coupling. There are some inexpensive Ni(II),<sup>17</sup> Fe(III),<sup>18</sup> Cu(0),<sup>19,20</sup> Cu(II)<sup>21</sup> and Cu(I)<sup>22</sup> catalysts for A<sup>3</sup>-coupling reactions. Namitharan and co-workers<sup>23</sup> employed Ni NPs as a catalyst for solvent free three-component coupling of aldehyde, alkyne and amine. In spite of their advantages, most of these catalytic systems often suffer from longer reaction time, high temperature and higher amount of catalyst and base.<sup>24</sup> In addition, some catalysts demonstrated poor reusability and stability, which made the

Received: June 17, 2015

Revised: August 8, 2015

Published: August 27, 2015



**Figure 1.** Schematic illustration for the preparation of CuO/GNS.

systems uneconomical. Recently, Cu NPs stabilized on MCM-41 were employed as an efficient catalyst for A<sup>3</sup>-coupling reactions but the system exhibited poor reusability of the catalyst.<sup>25</sup> To overcome these problems, an efficient, stable and a mild catalytic system for the A<sup>3</sup>-coupling reaction is obviously important.

Few-layer graphene nanosheets (GNS) have attracted tremendous attention due to their unique physicochemical properties such as high surface area, chemical stability, electrical conductivity and dispersion in solvents.<sup>26,27</sup> Immobilization of metal NPs on the surface of GNS was found to play a very useful role in different fields such as energy, biomedical, catalysis and sensors.<sup>28–30,18</sup> Particularly, the Cu NPs-decorated GNS are frequently utilized for various applications due to their outstanding activity.<sup>31,32</sup> For example, Fakhri et al.<sup>33</sup> prepared Cu NPs supported on graphene oxide via reduction method and found it as a highly active and recyclable catalyst for the synthesis of formamides and primary amines. Wang and co-workers<sup>34</sup> found that the decoration of CuO on graphene showed high performance as an anode material in lithium-ion batteries. Moreover, because the GNS are electrically conductive, they can hold the NPs in a highly dispersed state even after several uses and, therefore, they can exhibit good reusability and stability.<sup>35</sup> In spite of these advantages, only limited number of reports on Cu NPs-based GNS hybrids for organic reactions is available in the literature and, particularly, no report for A<sup>3</sup>-coupling reactions so far. In our opinion, the cost of GNS is one of the main issues that make them less affordable. Sustainable use of GNS after the catalytic process will make them viable and cost-effective. Herein we report a mild and highly efficient CuO/GNS-mediated catalytic system for A<sup>3</sup>-coupling reaction. The physicochemical characteristics of CuO/GNS were investigated by various techniques. The CuO/GNS hybrid was reused in the same and different (*aza*-Michael reaction of amines with acrylonitrile) reactions. The importance and reason for choosing *aza*-Michael reaction are discussed in the section *Versatility of the CuO/GNS*. Moreover, the GNS and CuO (as CuCl<sub>2</sub>) were successfully recovered from the used *μ*-CuO/GNS by a simple solution method.

## EXPERIMENTAL SECTION

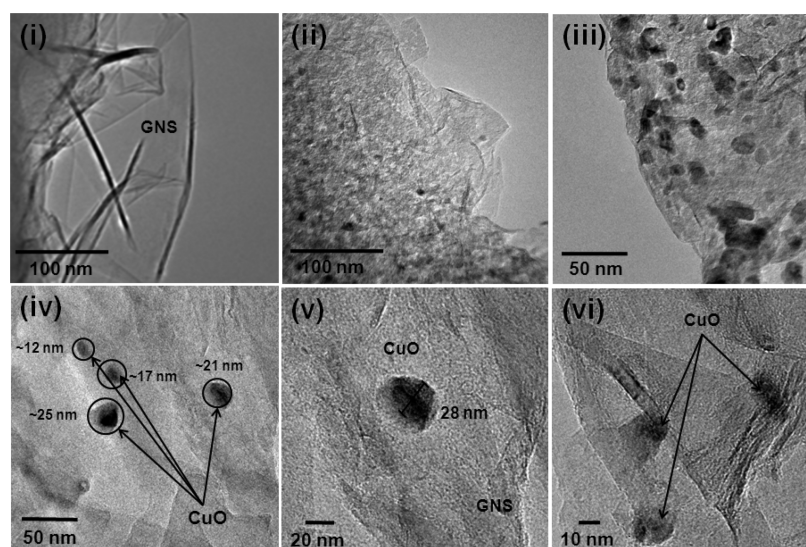
**Materials and Characterization.** High quality few-layer reduced graphene oxide (GO; purity, >99 %; surface area, >600 m<sup>2</sup>/g; thickness, ≤3.0 nm) was purchased from ACS Materials and used as received. Cu(acac)<sub>2</sub> (97%) was purchased from Wako Pure Chemicals. All other chemicals were purchased from Sigma-Aldrich or Wako Pure Chemicals.

Transmission electron microscopy (TEM) images were obtained on a JEOL JEM-2100F HR-TEM with the accelerating voltage of 200 kV.

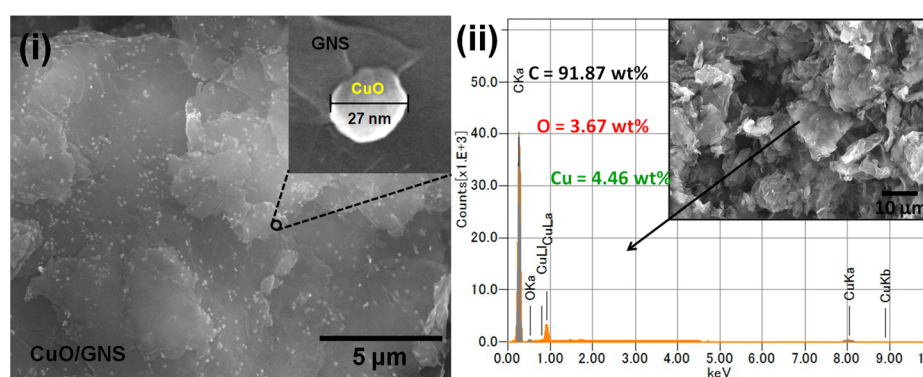
To quantify the weight percentage of Cu in CuO/GNS, scanning electron microscope-energy dispersive spectroscopy (SEM-EDS) measurement was recorded using a Hitachi 3000H SEM. The same field of view was then scanned using an EDS spectrometer to acquire a set of X-ray maps for Cu, C and O using 1 ms point acquisition for approximately one million counts. The weight percentage of Cu in the CuO/GNS was determined using inductively coupled plasma mass spectroscopy (ICP-MS, 7500CS, Agilent). Raman spectra were recorded on Hololab 5000, Kaiser Optical Systems Inc., USA to examine the interaction between CuO NPs and GNS. The Ar laser was operated at 532 nm with a Kaiser holographic edge filter. The X-ray diffraction (XRD) experiment was performed at room temperature using a Rotaflex RTP300 (Rigaku Co., Japan) diffractometer at 50 kV and 200 mA. Nickel-filtered Cu K $\alpha$  radiation ( $5 < 2\theta < 80^\circ$ ) was used for XRD measurements. X-ray photoelectron spectroscopy (XPS, Kratos Axis-Ultra DLD, Kratos Analytical Ltd., Japan) was recorded to confirm the chemical state of Cu in CuO/GNS. To confirm the formation of the product during catalysis, samples of reaction mixture were dissolved in ethyl acetate and then analyzed by gas chromatography (GC, Shimadzu GC-2014). The GC instrument was equipped with 5% diphenyl and 95% dimethylsiloxane, a Restek capillary column (0.32 mm dia, 60 m length) and a flame ionization detector (FID). He gas was used as a carrier gas. The initial column temperature was increased from 60 to 150 °C at the rate of 10 °C/min and then to 280 °C at the rate of 40 °C/min. During the product analyses, the temperatures of the FID and injection port were kept constant at 150 and 280 °C, respectively. The heterogeneity of the catalyst was tested using inductively coupled plasma-mass spectrometry (ICP-MS, 7500CS, Agilent). Nuclear magnetic resonance (NMR) spectra were recorded on a 400 MHz Bruker spectrometer using tetramethylsilane (TMS) as a standard.

**Preparation of CuO/GNS.** In a typical procedure, 1.0 g of graphene oxide (GO) was dispersed in methanol (MeOH) followed by ultrasonication for 1 h. Subsequently, 0.20 g of Cu(acac)<sub>2</sub> was added into the above prepared solution and stirred at 60 °C for 5 h in air atmosphere (step 1). After that, the MeOH was slowly evaporated and the resultant solid was mixed well by a mortar and pestle at ambient conditions for 30 min (step 2). Subsequently, the homogeneous mixture of GNS and Cu(acac)<sub>2</sub> was calcinated under nitrogen atmosphere at 350 °C for 3 h in a muffle furnace. **Figure 1** shows a schematic illustration of the procedure for the preparation of CuO/GNS. For comparison, the catalysts with different weight percentages were also prepared.

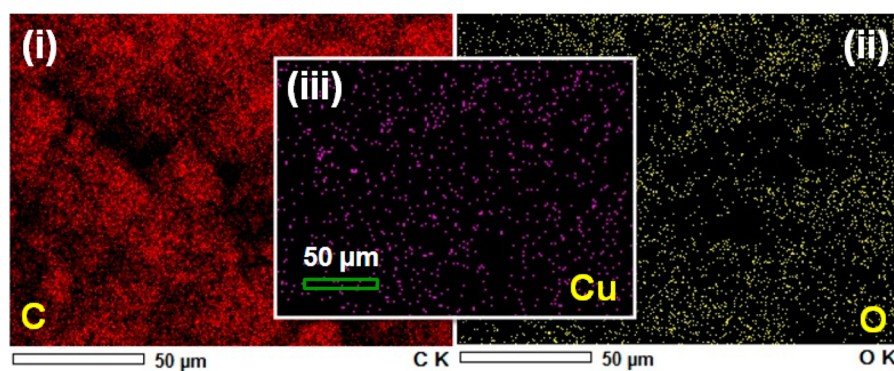
**Procedure for A<sup>3</sup>-Coupling Reaction.** CuO/GNS (10 mg, 0.7 mol % Cu) was added into a mixture of benzaldehyde (**1a**, 1 mmol), piperidine (**2a**, 1.2 mmol) and ethynyl benzene (**3a**, 1.5 mmol) in 5 mL of acetonitrile, and the solution was stirred under air atmosphere at 82 °C for 5 h. The progress of the reaction was monitored by GC. After the completion of the reaction, the CuO/GNS was separated out from the reaction mixture via centrifugation and then the separated CuO/GNS was washed well with diethyl ether and dried in an oven at 60 °C. The centrifugate was partitioned between 10 mL of ethyl acetate and 5 mL of saturated aqueous sodium hydrogen carbonate solutions. Then the ethyl acetate layer was separated out and dried



**Figure 2.** TEM images of (i) pure GO, (ii and iii) CuO/GNS and (iv, v and vi) magnified TEM images of CuO/GNS.



**Figure 3.** (i) FE-SEM image of CuO/GNS (inset: magnified FE-SEM image of CuO attached on GNS) and (ii) SEM image (inset) and corresponding EDS spectrum of CuO/GNS.



**Figure 4.** EDS elemental mappings of CuO/GNS: (i) C, (ii) O and (iii) Cu.

over anhydrous magnesium sulfate. Finally, the ethyl acetate layer was concentrated to obtain 1-(1,3-diphenylprop-2-yn-1-yl)piperidine (**4aaa**). The yield of product was determined by GC. Further, the product was isolated and confirmed by NMR spectroscopy.  $^1\text{H}$  NMR (400 MHz,  $\text{DMSO-}d_6$ ):  $\delta$  1.22–1.73 (m, 6H), 2.55 (t, 4H), 4.95 (s, 1H), 7.28–7.30 (m, 6H), 7.36–7.40 (m, 2H), 7.50–7.58 (m, 2H) ppm.  $^{13}\text{C}$  NMR (150 MHz,  $\text{DMSO-}d_6$ ):  $\delta$  24.42, 26.08, 50.42, 61.57, 86.38, 87.93, 122.82, 127.82, 128.46, 128.83, 129.02, 131.86, 138.73 ppm.

**Procedure for aza-Michael Reaction.** A mixture of piperidine (1 mmol) and acrylonitrile (1.2 mmol) was stirred in 5 mL of acetonitrile

in the presence of CuO/GNS (5 mg, 0.34 mol %) under atmospheric pressure of air at 25 °C for 1 h. The completion of the reaction was checked by TLC and GC analyses. Once the reaction completed, the catalyst was separated out from the reaction mixture by simple filtration and the products and unconverted reactants were analyzed by GC without any purification. The obtained 3-(piperidin-1-yl)propanenitrile was isolated and confirmed by NMR analysis.  $^1\text{H}$  NMR (400 MHz,  $\text{DMSO-}d_6$ ):  $\delta$  1.36–1.52 (m, 6H), 2.36 (t, 4H), 2.53 (t, 2H), 2.62 (t, 2H) ppm.  $^{13}\text{C}$  NMR (150 MHz,  $\text{DMSO-}d_6$ ):  $\delta$  15.30, 24.23, 25.81, 53.71, 53.86, 120.39 ppm.

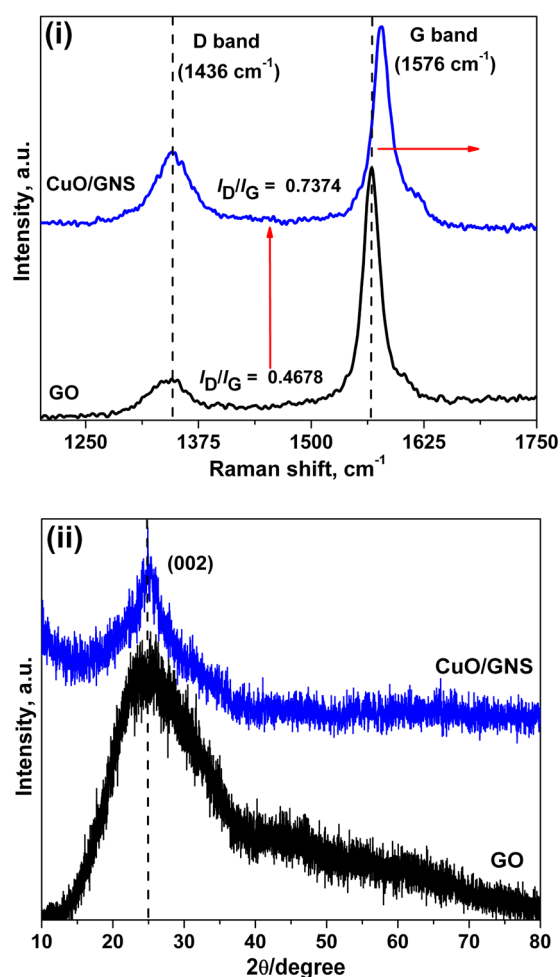
**Recovery of GNS from *u*-CuO/GNS.** Prior to the recovery process, the used nanocatalyst (*u*-CuO/GNS) was washed well with diethyl ether and dried at 60 °C for 3 h. A 50 mg of *u*-CuO/GNS was dispersed in conc. HCl followed by sonication for 10 min and stirring at 60 °C for 5 h. Then the hot mixture was filtered through a filter paper to recover the GNS. The filtrate was concentrated to collect the Cu in the form of CuCl<sub>2</sub>. Finally, the recovered GNS (*r*-GNS) was washed several times with conc. HCl and distilled water. The weight of the *r*-GNS was determined by weighing the filter paper after and before filtration. TEM, SEM-EDS, Raman and XPS analyses were followed to confirm the successful recovery of GNS.

## RESULTS AND DISCUSSION

**Characterization of CuO/GNS.** TEM images were taken to understand the surface morphology of GO and CuO/GNS; the images are presented in Figure 2. As shown in Figure 2i, the GO is a highly pure, continuous, wrinkled and transparent sheet with an average thickness of about 0.8–2 nm. Figure 2ii–vi confirms that the CuO NPs were homogeneously dispersed on the surface of the GNS. The average particle size of CuO NPs was found to be ca. ~26 nm. The high resolution TEM images [Figure 2v,vi] show the strong attachment of CuO NPs on the GNS with particle size distribution of 12–35 nm. See Figure S1 in the Supporting Information for more information. Figure 3 shows the FE-SEM image [Figure 3i] and SEM-EDS spectrum [Figure 3ii] of CuO/GNS. As with the TEM images, the FE-SEM image demonstrates the good dispersion of CuO NPs on GNS; more FE-SEM images are provided in Figure S2. The weight percentage of Cu in CuO/GNS was found to be 4.46 wt % [Figure 3ii]. The EDS elemental mapping of CuO/GNS [Figure 4i–iii] depicts the homogeneous distribution of CuO NPs in CuO/GNS. Moreover, only three elements (C, O and Cu) were observed in EDS spectrum, which proved the high purity of the CuO/GNS. ICP-MS was used to determine the weight percentage of Cu in CuO/GNS and it was found to be 4.37 wt %. The ICP-MS result agrees well with the EDS analysis.

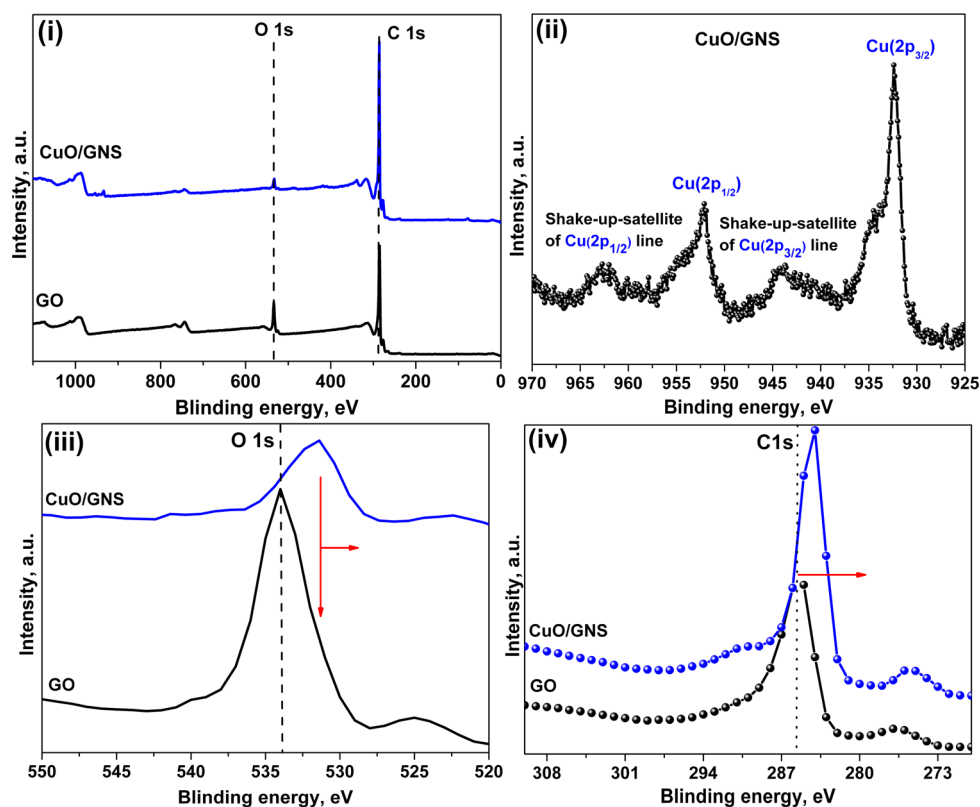
Raman spectra were recorded for GNS and CuO/GNS, under 514.5 nm excitation over the Raman shift interval of 250–4000 cm<sup>-1</sup> [Figure 5i]. As expected, both GNS and CuO/GNS exhibited two main Raman features, corresponding to the well-defined D-band line at ~1345 cm<sup>-1</sup> and G-band line at ~1570 cm<sup>-1</sup>.<sup>36</sup> The G-band line was originated from the in-plane vibration of sp<sup>2</sup> carbon atoms, which represented the relative degree of graphitization. The D-band line was related to the amount of disorder, which arises only in the presence of defects, indicating the presence of sp<sup>3</sup> carbon atoms or defect sites in graphene.<sup>37</sup> The intensity ratios of D and G bands ( $I_D/I_G$ ) were calculated. It is noteworthy that the  $I_D/I_G$  ratio (0.7374) of CuO/GNS was higher than that of GO (0.4678). Moreover, in comparison to GO, a positive shift in the G band (1576 to 1586 cm<sup>-1</sup>) was observed for CuO/GNS. These results indicate a strong attachment via covalent bonding between GO and CuO NPs (Cu–C).<sup>38</sup> Figure 5(ii) shows the XRD patterns of GO and CuO/GNS. A broad peak at 25° was observed for both GO and CuO/GNS, which was attributed to the (002) plane of the hexagonal graphite structure. Unfortunately, no other X-ray diffraction peaks correspond to the CuO NPs were found in CuO/GNS. This may be due to the very small size and nanocrystalline nature of the CuO NPs with lower weight percentage.<sup>30</sup>

To investigate further the oxidation state and weight percentage of Cu in CuO/GNS, XPS spectra were recorded for GO and CuO/GNS; the results are given in Figure 6. Both



**Figure 5.** (i) Raman spectra and (ii) XRD pattern of GO and CuO/GNS.

GO and CuO/GNS showed two dominant peaks at 284.5 and 533.5 eV, corresponding to C 1s and O 1s, respectively.<sup>39</sup> The O 1s peak of GO indicates the presence of oxygen functional groups such as carbonyl (C=O), carboxylic (–COOH), hydroxyl (C–OH) and ether (–C–O–C–), and H<sub>2</sub>O. However, the O 1s peak intensity dramatically decreased in CuO/GNS, which demonstrates the reduction of oxygen functional groups.<sup>40</sup> The Cu 2p XPS spectrum of CuO/GNS showed shakeup satellite peaks of the Cu 2p<sub>3/2</sub> at 942.4 and Cu 2p<sub>1/2</sub> at 962.6 eV, which confirmed the presence of Cu(II) species (CuO).<sup>41</sup> Similarly, the O 1s peak at 530.6 eV that corresponded to the photoemission of CuO was observed [Figure 6iii]. Generally, the characteristic shakeup satellite is peculiar to the Cu(II) species, which relates to d<sup>9</sup> configuration of Cu. Whereas, in the case of Cu<sub>2</sub>O, no satellite peaks can be observed; because the screening via a charge transfer into the d states is not possible due to the presence completely filled d shell.<sup>41</sup> Although the Cu is in the form of CuO, the main Cu 2p XPS peaks were observed at 932.7 eV (Cu 2p<sub>3/2</sub>) and 952.4 eV (Cu 2p<sub>1/2</sub>) with a spin–orbit splitting of ~19 eV. The binding energy (BE) of Cu 2p<sub>3/2</sub> and Cu 2p<sub>1/2</sub> is quite lower compared to the values previously reported for CuO.<sup>21,41</sup> This phenomenon is mainly due to the strong interaction of CuO NPs with GNS surface via covalent bonding (Cu–C).<sup>42</sup> Figure 6iv shows the C 1s peak of GO and CuO/GNS. It can be seen that the C 1s peak of CuO/GNS was shifted toward lower BE



**Figure 6.** (i) XPS survey spectrum of GO and CuO/GNS, (ii) Cu 2p XPS peak of CuO/GNS and (iii) O 1s peak and (iv) C 1s peak of GO and CuO/GNS.

**Table 1. Screening for Best Reaction Conditions<sup>a</sup>**

entry	solvent <sup>b</sup>	amount of catalyst (mol %)	temperature (°C)	time (h)	GC yield <sup>c</sup> (%)	(TON/TOF h <sup>-1</sup> ) <sup>d</sup>
1	DMF	0.7	82	5	14	20/4
2	methanol	0.7	82	5	41	59/12
3	acetonitrile	0.7	82	5	89	127/25
4	DMSO	0.7	82	5	15	21/4
5	ethanol	0.7	82	5	19	27/5
6	acetonitrile	0	82	5		
7	acetonitrile	5 mg (pure GNS)	82	5	trace	
8	acetonitrile	0.2	82	5	49	254/49
9	acetonitrile	0.5	82	5	68	136/27
10	acetonitrile	1.1	82	5	91	76/15
11	acetonitrile	0.7	25	5	trace	
12	acetonitrile	0.7	50	5	21	30/6
13	acetonitrile	0.7	70	5	41	58/12
14	acetonitrile	0.7	82	0.5	13	19/15
15	acetonitrile	0.7	82	1	19	27/27
16	acetonitrile	0.7	82	2	47	67/34
17	acetonitrile	0.7	82	3	56	80/27
18	acetonitrile	0.7	82	4	73	104/26
19	acetonitrile	0.7	82	6	89	127/21

<sup>a</sup>Reaction condition: aldehyde (1 mmol), amine (1.2 mmol), alkyne (1.5 mmol) were stirred with CuO/GNS in solvent at 82 °C. <sup>b</sup>5 mL aliquot of solvent was used in all the reactions. <sup>c</sup>GC yield. <sup>d</sup>TON/TOF [TON = the amount of product (mol)/the amount of active sites; TOF = TON/time (h)].

(from  $\sim 287$  to  $\sim 286$  eV) when compared to GO, indicating good dispersion of CuO NPs on GNS. Moreover, the weight percentage of Cu (4.61 wt %) in CuO/GNS was measured by XPS analysis. It is worth mention that the XPS spectrum of CuO/GNS confirmed the presence of only three elements (C, O and Cu). This observation acknowledges the reliability of the preparation process and purity of the catalyst. The XPS results are in good agreement with the XRD, TEM and SEM-EDS analyses.

The BET specific surface area was determined for GO and CuO/GNS. It was found that the CuO/GNS has a BET surface area of  $66.26 \text{ m}^2 \text{ g}^{-1}$  with a pore volume of  $0.2676 \text{ cm}^3 \text{ g}^{-1}$  and a BJH desorption average pore diameter of 16.15 nm. However, the surface area of CuO/GNS is significantly lower than that of pure GO ( $>600 \text{ m}^2/\text{g}$ ), which may be due to the face-to-face aggregation of graphene sheets. This value shows that about 60 graphene sheets aggregate into graphitic stacks that hinder intercalation of nitrogen. In fact, after the reduction of GO sheets, the reduced GO can easily aggregate due to the removal of oxygenated functional groups, mainly carboxylic ( $-\text{COOH}$ ) group, resulting in the loss in specific surface area. The results are in good agreement with a previous report.<sup>43</sup>

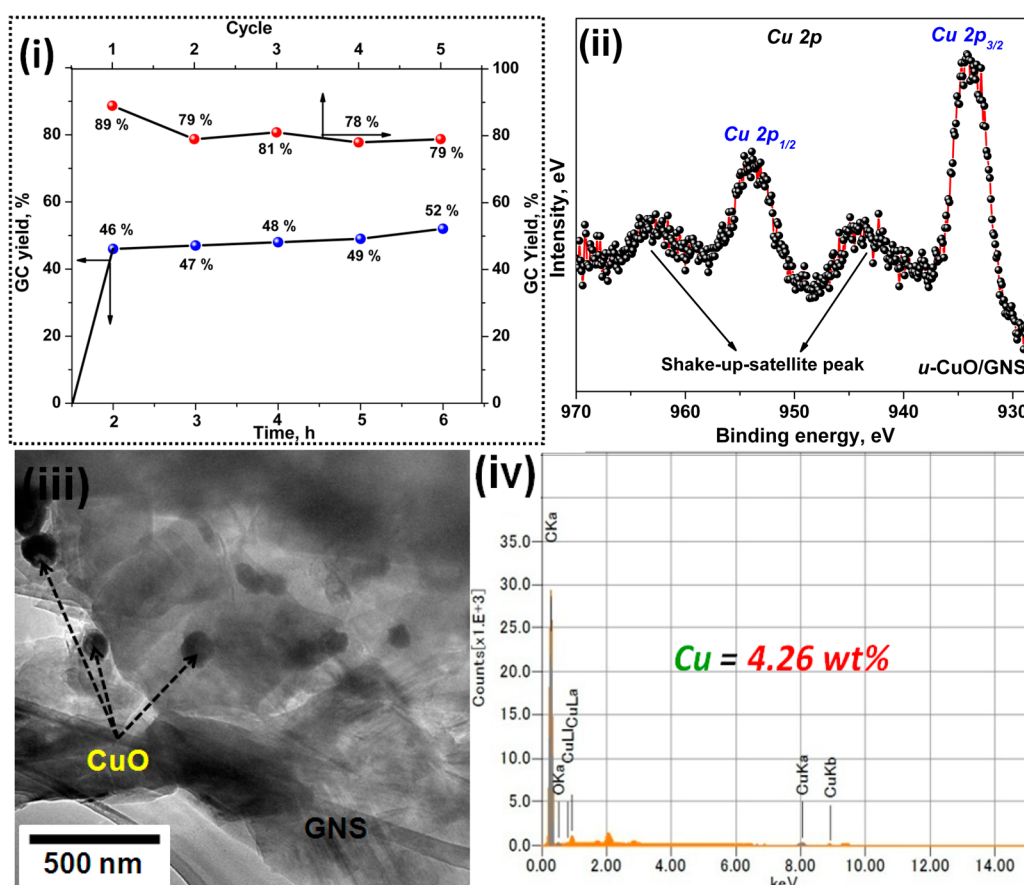
**Optimization of Reaction Conditions.** To find out the most suitable reaction conditions for  $A^3$ -coupling reactions, a series of reactions with different reaction parameters such as solvent, reaction time, temperature and catalyst amount was carried out (Table 1). Benzaldehyde (1a), piperidine (2a) and ethynyl benzene (3a) were chosen as model substrates for the optimization reactions. At first, various solvents such as *N,N*-dimethylformamide (DMF), acetonitrile, methanol, dimethyl sulfoxide (DMSO) and ethanol were examined (Table 1, entries 1–5). Among them, acetonitrile was found to be the best one with 89% yield of the desired product (4aaa) (Table 1, entry 3). As expected, no conversion was observed in the absence of CuO/GNS (Table 1, entry 6). Similarly, when the reaction was performed using GNS as a catalyst, only a trace amount of 4aaa was obtained (Table 1, entry 7). The amount of the catalyst played a crucial role in the reaction. It was found that 0.7 mol % of Cu (5 mg of CuO/GNS) is the optimum amount of the catalyst because it gave a better yield (89%) (Table 1, entry 3). Furthermore, no significant change in the yield was observed even after increasing the amount of catalyst to 1.1 mol % (Table 1, entry 10). However, decreasing the amount of catalyst (0.2 and 0.5 mol %) reduced the yield of 4aaa (Table 1, entries 8 and 9). Subsequently, reaction time was optimized. At room temperature ( $25^\circ\text{C}$ ), the reaction was very slow and gave only a trace amount of 4aaa (Table 1, entry 11). But, raising the reaction temperature gradually increases the yield of the product (Table 1, entries 12 and 13). An excellent 89% yield of 4aaa was formed when the reaction was performed at  $82^\circ\text{C}$  (Table 1, entry 3). In the time optimization, the progress of the reaction was monitored at 1 h intervals (Table 1, entries 14–19) and found that 5 h is the optimum reaction time. However, prolonged reaction (6 h) showed no change in the yield (89%) (Table 1, entry 19). Turnover number (TON) and turnover frequency (TOF) were calculated for the reactions using the equation given under Table 1. It is worth mention that the TON is 127 and TOF is  $25 \text{ h}^{-1}$  for the optimized reaction; the values are quite higher compared to those of previous reports on Cu NPs-catalyzed  $A^3$ -coupling reactions. These reaction conditions were adopted to extend the scope of the catalytic system.

**Scope of the Catalytic System.** A wide range of aromatic aldehydes, amines and alkynes were employed to extend the scope of the catalytic system (Table 2). The yield of  $A^3$ -coupled products ranged from 52% to 98%, depending on the substrates (Table 2). Coupling of benzaldehyde (1a), piperidine (2a) and ethynylbenzene (3a) gave 1-(1,3-diphenylprop-2-yn-1-yl)-piperidine (4aaa) in excellent 89% yield with good TON and TOF values of 126 and  $25 \text{ h}^{-1}$ , respectively. Whereas, the nano

**Table 2. Substrate Scope of the CuO/GNS-Catalyzed Three-Component Coupling of Aldehyde, Amine and Alkyne<sup>a</sup>**

$\text{R}_1\text{-CHO} + \text{R}_2\text{-NHR}_3 + \text{C}\equiv\text{C-R}_4 \xrightarrow[\text{C}_2\text{H}_5\text{N}, 82^\circ\text{C}]{\text{CuO/GNS (0.7 mol\%)}} \text{R}_1\text{-C}\equiv\text{C-C(R}_2\text{)-NHR}_3$			
1	2	3	4
			4aaa, (89%) <sup>b</sup> , (81%) <sup>c</sup> , 5 h, (126/25 h <sup>-1</sup> ) <sup>d</sup>
			4aac, (92%) <sup>b</sup> , (82%) <sup>c</sup> , 4.5 h, (132/29 h <sup>-1</sup> ) <sup>d</sup>
			4aae, (79%) <sup>b</sup> , 8 h, (113/14 h <sup>-1</sup> ) <sup>d</sup>
			4aad, (56%) <sup>b</sup> , 6 h, (80/14 h <sup>-1</sup> ) <sup>d</sup>
			4aab, (52%) <sup>b</sup> , 6 h, (75/13 h <sup>-1</sup> ) <sup>d</sup>
			4aba, (90%) <sup>b</sup> , (79%) <sup>c</sup> , 4 h, (129/32 h <sup>-1</sup> ) <sup>d</sup>
			4abc, (96%) <sup>b</sup> , (85%) <sup>c</sup> , 4 h, (137/35 h <sup>-1</sup> ) <sup>d</sup>
			4abb, (88%) <sup>b</sup> , (73%) <sup>c</sup> , 3.5 h, (126/36 h <sup>-1</sup> ) <sup>d</sup>
			4bac, (98%) <sup>b</sup> , (86%) <sup>c</sup> , 4.5 h, (140/31 h <sup>-1</sup> ) <sup>d</sup>
			4cac, (94%) <sup>b</sup> , (82%) <sup>c</sup> , 3.5 h, (135/39 h <sup>-1</sup> ) <sup>d</sup>
			4daa, (67%) <sup>b</sup> , 9 h, (96/11 h <sup>-1</sup> ) <sup>d</sup>
			4dab, (71%) <sup>b</sup> , 3 h, (102/34 h <sup>-1</sup> ) <sup>d</sup>
			4dac, (96%) <sup>b</sup> , (85%) <sup>c</sup> , 4.5 h, (137/31 h <sup>-1</sup> ) <sup>d</sup>
			4fba, (95%) <sup>b</sup> , (85%) <sup>c</sup> , 12 h, (136/12 h <sup>-1</sup> ) <sup>d</sup>
			4fbb, (87%) <sup>b</sup> , 5.5 h, (125/23 h <sup>-1</sup> ) <sup>d</sup>
			4fbc, (95%) <sup>b</sup> , (88%) <sup>c</sup> , 3.5 h, (136/39 h <sup>-1</sup> ) <sup>d</sup>
			4gba, (84%) <sup>b</sup> , 10 h, (120/12 h <sup>-1</sup> ) <sup>d</sup>
			4gbc, (96%) <sup>b</sup> , (89%) <sup>c</sup> , 5.5 h, (137/25 h <sup>-1</sup> ) <sup>d</sup>
			4daf, (63%) <sup>b</sup> , 6 h, (90/15 h <sup>-1</sup> ) <sup>d</sup>
			4eba, (88%) <sup>b</sup> , 3 h, (126/42 h <sup>-1</sup> ) <sup>d</sup>
			4ebc, (98%) <sup>b</sup> , 3 h, (140/47 h <sup>-1</sup> ) <sup>d</sup>

<sup>a</sup>Reaction conditions: aldehyde (1.0 mmol), amine (1.2 mmol), alkyne (1.5 mmol), CuO/GNS (0.7 mol %), acetonitrile (5 mL), air atmosphere, 3.5–12 h,  $82^\circ\text{C}$ . <sup>b</sup>GC yield with respect to aldehyde. <sup>c</sup>Isolated yield. <sup>d</sup>TON/TOF.



**Figure 7.** (i) Reusability and heterogeneity tests of CuO/GNS and, (ii) Cu 2p XPS peak, (iii) TEM image and (iv) EDS spectrum of *u*-CuO/GNS.

CuO-catalytic system afforded only 82% of the desired product at 90 °C even after 6 h.<sup>44</sup> It was noticed that the alkynes bearing either electron-donating or electron-withdrawing groups on the benzene ring are readily coupled with aldehydes and amines in moderate to excellent yields. For instance, 4-ethynylaniline (**3c**) reacted with **1a** and **2a** rapidly (4.5 h) and afforded the corresponding propargylamine (**4aac**) in excellent 92% yield with good TON/TOF (132/29 h<sup>-1</sup>). Similarly, a good 79% yield of **4aae** was obtained from the coupling of **1a**, **2a** and 1-ethynyl-4-fluorobenzene (**3e**). However, quite longer reaction times and moderate yields were observed for propargylamines **4aab** and **4aad**, prepared from 1-ethynyl-4-methylbenzene and 1-ethynyl-4-methoxybenzene, respectively. The A<sup>3</sup>-coupled product **4aba** derived from pyrrolidine (**2b**) was obtained in excellent yield of 90% with good TON/TOF (129/32 h<sup>-1</sup>). Alike, 96% **4abb** and 88% **4abc** were achieved from 1-ethynyl-4-methylbenzene and 4-ethynylaniline, respectively.

Aromatic aldehydes bearing either electron-donating or electron-withdrawing groups on the benzene ring were also investigated and found that it had a great influence on the yields. The electron-donating group substituted aldehydes reacted faster and gave good yields than the electron-withdrawing group substituted aldehydes. Reaction of 4-bromobenzaldehyde (**1b**), **2a** and **3c** gave the corresponding propargylamine (**4bac**) in excellent 98% yield with good TON/TOF values (140/31 h<sup>-1</sup>) after 4.5 h. Alike, propargylamine (**4cac**) derived from 4-chlorobenzaldehyde (**1c**) required comparatively less reaction time (3.5 h) to achieve 94% yield. 4-Methylbenzaldehyde (**1d**) coupled with **3a** or **3b** gave the

propargylamine **4daa** or **4dab** in moderate yield; even extended reaction time showed no significant improvement in the yield. Interestingly, a good 96% yield with excellent TON/TOF values (137/31 h<sup>-1</sup>) was obtained for the derivative of 4-methylbenzaldehyde (**4dac**). 3-Bromobenzaldehyde (**1f**) and **2b** were reacted with different alkynes such as **3a**, **3b** and **3c** to form the corresponding A<sup>3</sup>-products **4fba**, **4fbb** and **4fbc** in good yields of 95%, 87% and 95%, respectively. Propargylamines **4gba** and **4gbc** were obtained in excellent yields (84 and 96%) from the coupling of 3-chlorobenzaldehyde (**1g**) and **2b** with **3a** and **3c**, respectively.

The present catalytic system is also efficient for the sterically hindered substrates such as 9-ethynyl-9H-fluoren-9-ol (**3f**) and pyrene-1-carbaldehyde (**1e**). The compounds **1e** and **2b** were readily coupled with different alkynes such as **3a** and **3c**, and produced the corresponding propargylamines (**4eba** and **4ebc**) in good yields (88% and 98%). A moderate yield of 63% was observed for **4daf** from the coupling of **1d**, **2a** and **3f**.

The results are well comparable with other reported heterogeneous Cu-based catalysts. For instance, Albaladejo et al.<sup>21</sup> showed that Cu<sub>2</sub>O/TiO<sub>2</sub> catalyzed A<sup>3</sup>-coupling and the yield of propargylamines varies from 52% to 98% with good TOF/TOF values (198–104/90–0.1 h<sup>-1</sup>). Similarly, Cu modified spherical MCM-41 nanoparticles gave the propargylamines in excellent yields (75–93%) with moderate TON/TOF (32–26/21–78 h<sup>-1</sup>).<sup>25</sup> Borah et al.<sup>19</sup> reported Cu(0)-nanoparticles stabilized on modified montmorillonite for A<sup>3</sup>-coupling reaction and the yield varied from 52% to 98% with excellent TON/TOF values (1640–1880/547–627 h<sup>-1</sup>). Recently, MCM-41 silica modified Cu(I)-thiosalen complex

has been reported for A<sup>3</sup>-coupling reactions. The yield of A<sup>3</sup>-coupled products ranged from 93 to 81% with very high TON/TOF values of 31 000–27 000/7750–2700 h<sup>-1</sup>.<sup>45</sup> Under solvent free conditions, nano Cu<sub>2</sub>O–ZnO catalyzed coupling of aldehydes or ketones, secondary amines, and terminal alkynes gave the coupled products in good yields (95–0%).<sup>46</sup> Mandal and co-workers prepared magnetically recoverable Fe<sub>3</sub>O<sub>4</sub>–GO nanocomposites for the A<sup>3</sup>-coupling reactions. They found that the nanocomposite is good, reusable and stable in terms of yields (93–37%) and TON/TOF values (310–123/19–8 h<sup>-1</sup>).<sup>47</sup> The present CuO/GNS system obtained the coupling products in excellent yields ranged from 98 to 52% with good TON/TOF values (140–75/47–11 h<sup>-1</sup>).

To explore further the present CuO/GNS catalyst, N-oxidation of tertiary amines was carried out. To the best of our knowledge, this is the first report on CuO NPs catalyzed N-oxidation of tertiary amines. Without any doubt, the N-oxidation reaction is one of the important organic reactions and the products (amine N-oxides) have found to play a key role in the preparation of various cosmetic products.<sup>48</sup> The reaction conditions for the N-oxidation reaction were adopted from one of our previously reported results.<sup>49</sup> Briefly, a mixture of amine (2 mmol), H<sub>2</sub>O<sub>2</sub> (5 mmol) and 5 mg of CuO/GNS was stirred with 5 mL of CH<sub>3</sub>CN under atmospheric pressure of air at 80 °C for 4 h (see the Supporting Information for detail). The completion of the reaction was monitored by TLC and the products were confirmed by NMR. Aliphatic tertiary amine, triethylamine, gave the corresponding N-oxide in an excellent yield of 98% with TON/TOF of 140/35 h<sup>-1</sup>. Similarly, 97% of *N,N*-dimethyl aniline N-oxide with good TON/TOF values (139/35 h<sup>-1</sup>) was obtained from the oxidation of *N,N*-dimethyl aniline. The results are better compared to those of some of the previously reported catalytic systems such as GNPs–RuO<sub>2</sub>NRs, Pt/C and Ti–MCM-41.<sup>49–51</sup>

#### Heterogeneity, Reusability and Stability of CuO/GNS.


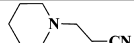

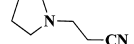
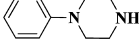
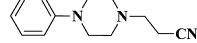
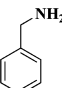
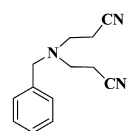
To understand the nature of the catalytic system, a heterogeneity test was performed for CuO/GNS. In a typical experiment, a mixture of benzaldehyde (**1a**, 1 mmol), piperidine (**2a**, 1.2 mmol) and ethynyl benzene (**3a**, 1.5 mmol) was stirred under the optimized reaction conditions for 2 h and the GC yield was found to be 47%. Subsequently, the catalyst was separated out by simple centrifugation and the filtrate was further stirred for 4 h without the catalyst. The progress of the reaction was monitored by GC at 2 h intervals, and the results are presented in Figure 7i. It was observed that there was no significant increase in the yield after the removal of CuO/GNS from the reaction mixture. The results confirmed that the reaction occurred only in the presence of the catalyst and CuO was not leached out from CuO/GNS during the coupling reaction.

The recyclability of the CuO/GNS was tested for the A<sup>3</sup>-coupling reaction of benzaldehyde (**1a**, 1 mmol), piperidine (**2a**, 1.2 mmol) and ethynyl benzene (**3a**, 1.5 mmol). After each cycle, the catalyst was recovered by simple centrifugation and washed with diethyl ether followed by drying under air atmosphere at 60 °C. The catalyst can be reused for five times without a significant loss of the yield. A good yield of 79% with high TON/TOF values (113/23 h<sup>-1</sup>) was observed even after the fifth cycle. The physicochemical stability of the CuO/GNS after use (1 cycle) was investigated in terms of XPS, TEM and EDS analyses [Figure 7ii–iv]. It can be seen that the morphology of the used CuO/GNS was maintained without

any significant aggregation of CuO NPs. As with pure CuO/GNS, the Cu 2p XPS spectrum of *u*-CuO/GNS also showed the shakeup satellite peaks of Cu 2p<sub>3/2</sub> at ~942 eV and Cu 2p<sub>1/2</sub> at ~962 eV, indicating an excellent chemical stability of the CuO/GNS. Moreover, the EDS spectrum showed that the weight percentage of Cu in *u*-CuO/GNS was 4.26 wt %. The corresponding elemental mapping showed a fine dispersion of CuO NPs (see Figure S3 in the Supporting Information). The stability of CuO/GNS even after fifth use was tested by using TEM, SEM-EDS and XPS (see Figure S5 in the Supporting Information). TEM image of CuO/GNS after fifth use shows that the size of CuO NPs is slightly increased by 10 to 15 nm (see Figure S5 in the Supporting Information). However, no significant change was observed in the oxidation state (+2) and weight percentage (4.19 wt %) of CuO NPs in CuO/GNS even after fifth use when compared to the fresh CuO/GNS catalyst (see Figure S5 in the Supporting Information). The results confirmed that the present CuO/GNS is heterogeneous, reusable and stable.

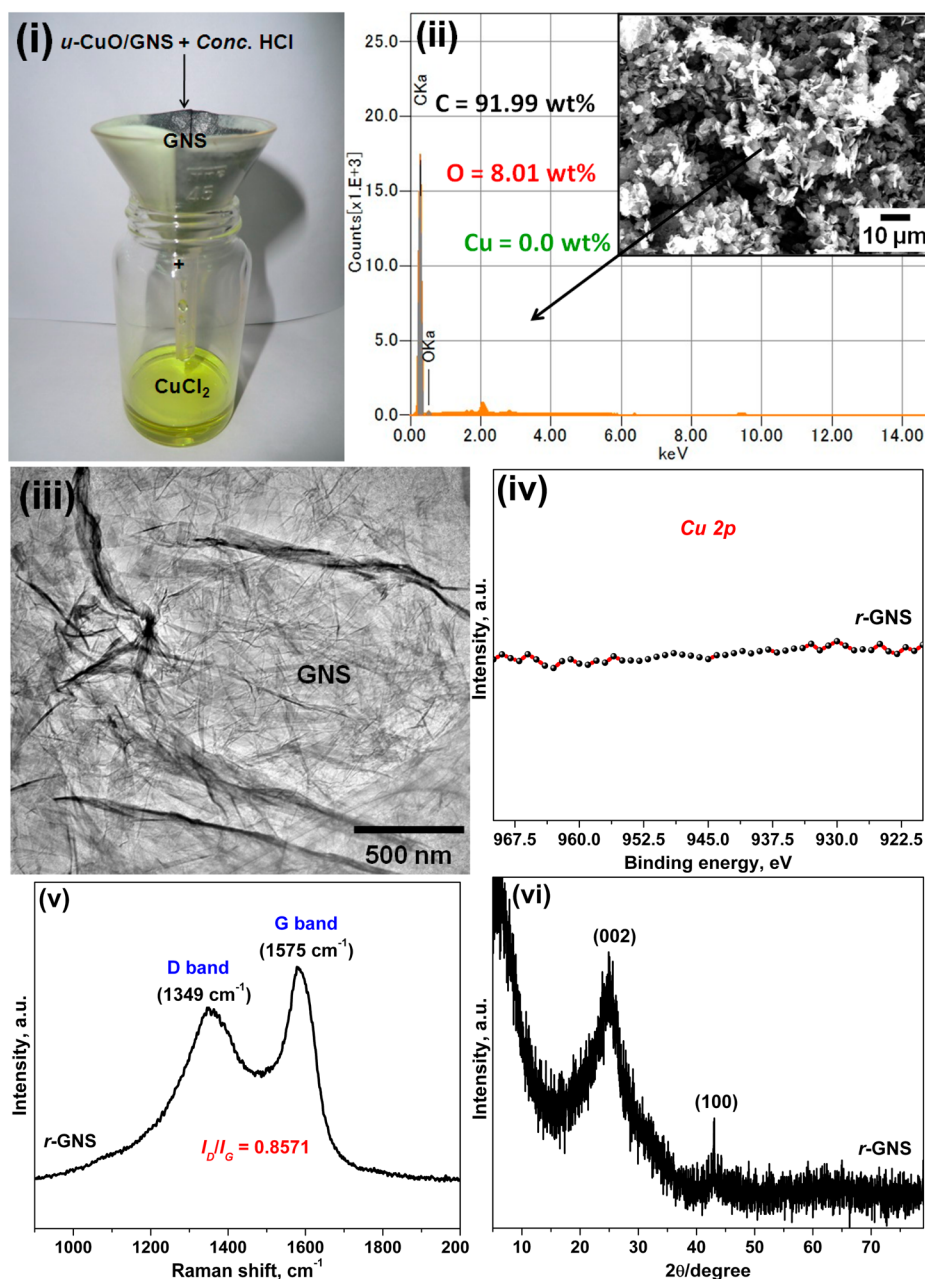
**Versatility of the CuO/GNS.** Encouraged by the good physicochemical stability of the catalyst after use (*u*-CuO/GNS), the *u*-CuO/GNS was further applied in *aza*-Michael reaction of amines with acrylonitrile. In fact, the β-amino carbonyl compounds are versatile class of intermediates and often utilized as a precursor in the synthesis of natural products, chiral auxiliaries, and antibiotics.<sup>52,53</sup> Initially, reaction conditions were optimized. For the screening, acrylonitrile and piperidine were chosen as model substrates. A low yield of the product (65%) was observed in the absence of *u*-CuO/GNS. Among the solvents optimized, acetonitrile was the best one since it afforded an excellent of 94%. A small amount of catalyst (5 mg, 0.34 mol % of Cu) was sufficient for the reaction. It was found that the optimum reaction time was 1 h. Under the optimized reaction conditions, the coupling between acrylonitrile and piperidine gave a better 94% yield of 3-(piperidin-1-yl)propanenitrile with high TON/TOF values (277/277 h<sup>-1</sup>) (Table 3, entry 1) whereas the nano CuO-catalytic system afforded only 85% yield of the desired product after 3 h.<sup>54</sup> An excellent 95% yield was observed in the coupling of pyrrolidine with acrylonitrile (Table 3, entry 2). Similarly, the present catalytic system obtained 88% of 3-(4-phenylpiperazin-1-yl)propanenitrile (Table 3, entry 3). Interestingly, primary

**Table 3.** *aza*-Michael Reaction of Amines with Acrylonitrile Catalyzed by *u*-CuO/GNS<sup>a</sup>

entry	amine	product	yield (%)	TON/TOF h <sup>-1</sup>
1			94 <sup>b</sup> (90) <sup>c</sup>	277/277
2			95 <sup>b</sup> (91) <sup>c</sup>	279/279
3			88 <sup>b</sup> (88) <sup>c</sup>	259/259
4 <sup>e</sup>			87 <sup>b</sup> (81) <sup>c</sup>	256/256

<sup>a</sup>Reaction conditions: amine (1.0 mmol), acrylonitrile (1.0 mmol), *u*-CuO/GNS (0.34 mol %), acetonitrile (5 mL), air atmosphere, 1 h, 25 °C. <sup>b</sup>GC yield. <sup>c</sup>Isolated yield. <sup>d</sup>TON/TOF. <sup>e</sup>2 mmol of acrylonitrile was used.





**Figure 8.** (i) Photographic image showing the recovery of GNS, (ii) EDS spectrum (inset: corresponding SEM image), (iii) TEM image, (vi) XPS Cu 2p peak, (v) Raman spectrum and (vi) XRD spectrum of the *r*-GNS.

amines were also actively coupled with alkenes. Bis adduct was formed in good 87% yield when phenylmethanamine was used as an amine (Table 3, entry 4). The results clearly showed the versatile nature of the CuO/GNS catalyst. More interestingly, the *u*-CuO/GNS was reused four times. After the fourth cycle, the reaction gave a good 81% yield of 3-(piperidin-1-yl)propanenitrile.

**Recovery of Graphene and CuO from *u*-CuO/GNS.** The sustainable use of the raw materials is very important to make the catalyst more economical. To prove this, we attempted to recover the graphene and also the metal nanoparticles (as CuCl<sub>2</sub>) from the *u*-CuO/GNS. The detailed recovery procedure is given in the Experimental Section. Figure 8i shows the photographic image of the recovery of graphene and CuCl<sub>2</sub>. It is interesting to note that the recovery of GNS was ~95%, and the CuO NPs were completely recovered as CuCl<sub>2</sub>.

The EDS spectrum [Figure 8(ii)] and its corresponding elemental mapping images (see Figure S4 in the Supporting Information) confirmed the complete removal of CuO NPs and the high purity of *r*-GNS. The TEM image of *r*-GNS also showed pure, continuous and wrinkled morphology without any CuO NPs. The mean thickness of the *r*-GNS sheet was calculated to be about 0.8–2 nm [Figure 8iii]. The Cu 2p peak completely disappeared in the XPS spectrum of *r*-GNS and the weight percentage was estimated to be 0%. Raman spectrum showed a characteristic D band at 1349 cm<sup>-1</sup> and G band at 1575 cm<sup>-1</sup>. However, the calculated I<sub>D</sub>/I<sub>G</sub> ratio was slightly higher (0.8571) than that of pure GO (0.5287), indicating the presence of more defect sites.<sup>55</sup> The defect sites might have been caused by the oxidation due to acid used in the recovery process. Interestingly, when compared to pure CuO/GNS, the *r*-GNS showed a better BET surface area of 110.11 m<sup>2</sup>/g. The

formation of more oxygen functional groups during the recovery process might be the reason for the better surface area. In fact, the oxygen functional groups on graphene can prevent the aggregation of graphene layers. In Figure Svi, the *r*-GNS exhibited a strong (002) diffraction peak at 26° and a (100) diffraction peak at 44.5°, corresponding to graphitic structure.<sup>56</sup> Furthermore, the recovered CuO NPs (as CuCl<sub>2</sub>) were investigated by the XPS analysis (see Figure S6 in the Supporting Information). In addition to the Cl 2p peak at ~200 eV, the Cu 2p peaks (Cu 2p<sub>3/2</sub> and Cu 2p<sub>1/2</sub>) and their corresponding shakeup satellite peaks were also observed, which proved the conversion of CuO NPs to CuCl<sub>2</sub>.<sup>57</sup> The result confirmed the successful recovery of GNS with its natural physicochemical properties. The recovered GNS and Cu may be used for further applications and, therefore, the present catalyst is viable.

**Conclusions.** In conclusion, a very simple and efficient method was developed to prepare the CuO/GNS nanocatalyst. The CuO/GNS demonstrated outstanding catalytic activity in terms of yield and TON/TOF toward A<sup>3</sup>-coupling reaction under mild, base free reaction conditions. The catalyst is heterogeneous, stable and reusable. The versatility of CuO/GNS was realized from the higher yield of *u*-CuO/GNS in *aza*-Michael reaction. Finally, the GNS and CuO NPs (as CuCl<sub>2</sub>) were successfully recovered from the *u*-CuO/GNS. The recovered *r*-GNS and CuCl<sub>2</sub> may be used for other applications. Overall, the simple preparation, outstanding activity, reusability, versatility and most importantly the sustainable use of raw materials make the heterogeneous CuO/GNS a most preferable one over the existing Cu-based catalysts for A<sup>3</sup>-coupling and *aza*-Michael reactions.

## ■ ASSOCIATED CONTENT

### 📄 Supporting Information

The Supporting Information is available free of charge on the ACS Publications website at DOI: 10.1021/acssuschemeng.5b00542.

TEM images, FE-SEM images, EDS elemental mappings, and XPS and NMR spectra (PDF).

## ■ AUTHOR INFORMATION

### Corresponding Authors

\*Ick Soo Kim. Phone: +81 268 21 5139. E-mail: kim@shinshu-u.ac.jp.

\*Ramasamy Karvembu. Phone: +91 431 2503636. E-mail: kar@nitt.edu.

### Notes

The authors declare no competing financial interest.

## ■ REFERENCES

- (1) Mandel, S.; Weinreb, O.; Amit, T.; Youdim, M. B. H. Mechanism of neuroprotective action of the anti-Parkinson drug rasagiline and its derivatives. *Brain Res. Rev.* **2005**, *48*, 379–387.
- (2) Weinreb, O.; Amit, T.; Bar-Am, O.; Youdim, M. B. H. Rasagiline: A novel anti-Parkinsonian monoamine oxidase-B inhibitor with neuroprotective activity. *Prog. Neurobiol.* **2010**, *92*, 330–344.
- (3) Binda, C.; Hubalek, F.; Li, M.; Herzig, Y.; Sterling, J.; Edmondson, D. E.; Mattevi, A. Crystal structures of monoamine oxidase B in complex with four inhibitors of the N-propargylaminoindan class. *J. Med. Chem.* **2004**, *47*, 1767–1774.
- (4) Murai, T.; Mutoh, Y.; Ohta, Y.; Murakami, M. Synthesis of tertiary propargylamines by sequential reactions of in situ generated

thioiminium salts with organolithium and-magnesium reagents. *J. Am. Chem. Soc.* **2004**, *126*, 5968–5969.

(5) Jung, M. E.; Huang, A. Use of optically active cyclic *N,N*-dialkyl amines in asymmetric induction. *Org. Lett.* **2000**, *2*, 2659–2661.

(6) Domling, A.; Wang, W.; Wang, K. Chemistry and biology of multicomponent reactions. *Chem. Rev.* **2012**, *112*, 3083–3135.

(7) Patil, M. K.; Keller, M.; Reddy, B. M.; Pale, P.; Sommer, J. Copper zeolites as green catalysts for multicomponent reactions of aldehydes, terminal alkynes and amines: An efficient and green synthesis of propargylamines. *Eur. J. Org. Chem.* **2008**, *2008*, 4440–4445.

(8) Peshkov, V. A.; Pereshivko, O. P.; Van der Eycken, E. V. A walk around the A<sup>3</sup>-coupling. *Chem. Soc. Rev.* **2012**, *41*, 3790–3807.

(9) Lo, V. K. Y.; Liu, Y.; Wong, M. K.; Che, C. M. Gold (III) salen complex-catalyzed synthesis of propargylamines via a three-component coupling reaction. *Org. Lett.* **2006**, *8*, 1529–1532.

(10) Wei, C.; Li, C. J. A highly efficient three-component coupling of aldehyde, alkyne, and amines via CH activation catalyzed by gold in water. *J. Am. Chem. Soc.* **2003**, *125*, 9584–9585.

(11) Pin-Hua, L.; Lei, W. Mercurous chloride catalyzed Mannich condensation of terminal alkynes with secondary amines and aldehydes. *Chin. J. Chem.* **2005**, *23*, 1076–1080.

(12) Zhang, Y.; Santos, A. M.; Herdtweck, E.; Mink, J.; Kuhn, F. E. Organonitrile ligated silver complexes with perfluorinated weakly coordinating anions and their catalytic application for coupling reactions. *New J. Chem.* **2005**, *29*, 366–370.

(13) Fodor, A.; Kiss, A.; Debreczeni, N.; Hell, Z.; Gresits, I. A simple method for the preparation of propargylamines using molecular sieve modified with copper (II). *Org. Biomol. Chem.* **2010**, *8*, 4575–4581.

(14) Villaverde, G.; Corma, A.; Iglesias, M.; Sanchez, F. Heterogenized gold complexes: recoverable catalysts for multicomponent reactions of aldehydes, terminal alkynes, and amines. *ACS Catal.* **2012**, *2*, 399–406.

(15) Zhang, X.; Corma, A. Supported gold (III) catalysts for highly efficient three-component coupling reactions. *Angew. Chem., Int. Ed.* **2008**, *47*, 4358–4361.

(16) Reddy, K. M.; Babu, N. S.; Prasad, P. S. S.; Lingaiah, N. The silver salt of 12-tungstophosphoric acid: an efficient catalyst for the three-component coupling of an aldehyde, an amine and an alkyne. *Tetrahedron Lett.* **2006**, *47*, 7563–7566.

(17) Lanke, S. R.; Bhanage, B. M. Nickel-catalyzed three-component coupling reaction of terminal alkynes, dihalomethane and amines to propargylamines. *Appl. Organomet. Chem.* **2013**, *27*, 729–733.

(18) Huo, X.; Liu, J.; Wang, B.; Zhang, H.; Yang, Z.; She, X.; Xi, P. A one-step method to produce graphene-Fe<sub>3</sub>O<sub>4</sub> composites and their excellent catalytic activities for three-component coupling of aldehyde, alkyne and amine. *J. Mater. Chem. A* **2013**, *1*, 651–656.

(19) Borah, B. J.; Borah, S. J.; Saikia, L.; Dutta, D. K. Efficient three-component coupling reactions catalyzed by Cu<sup>0</sup>-nanoparticles stabilized on modified montmorillonite. *Catal. Sci. Technol.* **2014**, *4*, 1047–1054.

(20) Guo, H.; Liu, X.; Xie, Q.; Wang, L.; Peng, D. L.; Branco, P. S.; Gawande, M. B. Disproportionation route to monodispersed copper nanoparticles for the catalytic synthesis of propargylamines. *RSC Adv.* **2013**, *3*, 19812–19815.

(21) Albaladejo, M. J.; Alonso, F.; Moglie, Y.; Yus, M. Three-component coupling of aldehydes, amines, and alkynes catalyzed by oxidized copper nanoparticles on titania. *Eur. J. Org. Chem.* **2012**, *2012*, 3093–3104.

(22) Wang, M.; Li, P.; Wang, L. Silica-immobilized NHC-Cu<sup>I</sup> complex: an efficient and reusable catalyst for A<sup>3</sup>-coupling (aldehyde-alkyne-amine) under solventless reaction conditions. *Eur. J. Org. Chem.* **2008**, *2008*, 2255–2261.

(23) Namitharan, K.; Pitchumani, K. Nickel-catalyzed solvent-free three-component coupling of aldehyde, alkyne and amine. *Eur. J. Org. Chem.* **2010**, *2010*, 411–415.

(24) Dulle, J.; Thirunavukkarasu, K.; Mittelmeijer-Hazeleger, M. C.; Andreeva, D. V.; Shiju, N. R.; Rothenberg, G. Efficient three-

component coupling catalysed by mesoporous copper–aluminum based nanocomposites. *Green Chem.* **2013**, *15*, 1238–1243.

(25) Abdollahi-Alibeik, M.; Moaddeli, A. Copper modified spherical MCM-41 nano particles: an efficient catalyst for the three-component coupling of aldehydes, amines and alkynes in solvent-free conditions. *RSC Adv.* **2014**, *4*, 39759–39766.

(26) Dreyer, D. R.; Park, S.; Bielawski, C. W.; Ruoff, R. S. The chemistry of graphene oxide. *Chem. Soc. Rev.* **2010**, *39*, 228–240.

(27) Georgakilas, V.; Otyepka, M.; Bourlinos, A. B.; Chandra, V.; Kim, N.; Kemp, K. C.; Hobza, P.; Zboril, R.; Kim, K. S. Functionalization of graphene: covalent and non-covalent approaches, derivatives and applications. *Chem. Rev.* **2012**, *112*, 6156–6214.

(28) Xu, C.; Wang, X.; Zhu, J. Graphene-metal particle nanocomposites. *J. Phys. Chem. C* **2008**, *112*, 19841–19845.

(29) Gopiraman, M.; Ganesh Babu, S.; Khatri, Z.; Kim, B. S.; Wei, K.; Karvembu, R.; Kim, I. S. Photodegradation of dyes by a novel TiO<sub>2</sub>/u-RuO<sub>2</sub>/GNS nanocatalyst derived from Ru/GNS after its use as a catalyst in the aerial oxidation of primary alcohols (GNS = graphene nanosheets). *Reac. Kinet. Mech. Cat.* **2015**, *115*, 759–772.

(30) Zhu, J.; Zeng, G.; Nie, F.; Xu, X.; Chen, S.; Han, Q.; Wang, X. Decorating graphene oxide with CuO nanoparticles in a water–isopropanol system. *Nanoscale* **2010**, *2*, 988–994.

(31) Gopiraman, M.; Ganesh Babu, S.; Khatri, Z.; Kai, W.; Kim, Y. A.; Endo, M.; Karvembu, R.; Kim, I. S. Dry synthesis of easily tunable nano ruthenium supported on graphene: novel nanocatalysts for aerial oxidation of alcohols and transfer hydrogenation of ketones. *J. Phys. Chem. C* **2013**, *117*, 23582–23596.

(32) Li, N.; Wang, Z.; Zhao, K.; Shi, Z.; Xu, S.; Gu, Z. J. Graphene-CuO nanocomposite. *J. Nanosci. Nanotechnol.* **2010**, *10*, 6690–6693.

(33) Fakhri, P.; Jaleh, B.; Nasrollahzadeh, M. Synthesis and characterization of copper nanoparticles supported on reduced graphene oxide as a highly active and recyclable catalyst for the synthesis of formamides and primary amines. *J. Mol. Catal. A: Chem.* **2014**, *383–384*, 17–22.

(34) Wang, B.; Wu, X. L.; Shu, C.Y.; Guo, Y. G.; Wang, C. R. Synthesis of CuO/graphene nanocomposite as a high-performance anode material for lithium-ion batteries. *J. Mater. Chem.* **2010**, *20*, 10661–10664.

(35) Singh, V.; Joung, D.; Zhai, L.; Das, S.; Khondaker, S. I.; Seal, S. Graphene based materials: past, present and future. *Prog. Mater. Sci.* **2011**, *56*, 1178–1271.

(36) Ferrari, A. C.; Basko, D. M. Raman spectroscopy as a versatile tool for studying the properties of graphene. *Nat. Nanotechnol.* **2013**, *8*, 235–246.

(37) Ni, Z.; Wang, Y.; Yu, T.; Shen, Z. Raman spectroscopy and imaging of graphene. *Nano Res.* **2008**, *1*, 273–291.

(38) Liu, Y.; Wang, W.; Gu, L.; Wang, Y.; Ying, Y.; Mao, Y.; Peng, X. Flexible CuO nanosheets/reduced-graphene oxide composite paper: binder-free anode for high-performance lithium-ion batteries. *ACS Appl. Mater. Interfaces* **2013**, *5*, 9850–9855.

(39) Gopiraman, M.; Ganesh Babu, S.; Khatri, Z.; Wei, K.; Endo, M.; Karvembu, R.; Kim, I. S. Facile and homogeneous decoration of RuO<sub>2</sub> nanorods on graphene nanoplatelets for transfer hydrogenation of carbonyl compounds. *Catal. Sci. Technol.* **2013**, *3*, 1485–1489.

(40) Gopiraman, M.; Karvembu, R.; Kim, I. S. Highly active, selective, and reusable RuO<sub>2</sub>/SWCNT catalyst for Heck olefination of aryl halides. *ACS Catal.* **2014**, *4*, 2118–2129.

(41) Gopiraman, M.; Ganesh Babu, S.; Khatri, Z.; Kai, W.; Kim, Y. A.; Endo, M.; Karvembu, R.; Kim, I. S. An efficient, reusable copper-oxide/carbon-nanotube catalyst for *N*-arylation of imidazole. *Carbon* **2013**, *62*, 135–148.

(42) Li, J.; Guo, L.; Zhang, L.; Yu, C.; Yu, L.; Jiang, P.; Wei, C.; Qin, F.; Shi, J. Donor- $\pi$ -acceptor structure between Ag nanoparticles and azobenzene chromophore and its enhanced third-order optical non-linearity. *Dalton Trans.* **2009**, 823–831.

(43) Si, Y.; Samulski, E. T. Exfoliated graphene separated by platinum nanoparticles. *Chem. Mater.* **2008**, *20*, 6792–6797.

(44) Kantam, M. L.; Laha, S.; Yadav, J.; Bhargava, S. An efficient synthesis of propargylamines via three-component coupling of

aldehydes, amines and alkynes catalyzed by nanocrystalline copper (II) oxide. *Tetrahedron Lett.* **2008**, *49*, 3083–3086.

(45) Naeimi, H.; Moradian, M. Copper(I)-N<sub>2</sub>S<sub>2</sub>-salen type complex covalently anchored onto MCM-41 silica: an efficient and reusable catalyst for the A<sub>3</sub>-coupling reaction toward propargylamines. *Appl. Organomet. Chem.* **2013**, *27*, 300–306.

(46) Hosseini-Sarvari, M.; Moeini, F. Nano copper(I) oxide–zinc oxide catalyzed coupling of aldehydes or ketones, secondary amines, and terminal alkynes in solvent-free conditions. *New J. Chem.* **2014**, *38*, 624–635.

(47) Mandal, P.; Chattopadhyay, A. P. Excellent catalytic activity of magnetically recoverable Fe<sub>3</sub>O<sub>4</sub>-graphene oxide nanocomposites prepared by a simple method. *Dalton Trans.* **2015**, *44*, 11444–11456.

(48) Boyer, J. H. Increasing the index of covalent oxygen bonding at nitrogen attached to carbon. *Chem. Rev.* **1980**, *80*, 495–561.

(49) Gopiraman, M.; Bang, H.; Ganesh Babu, S.; Wei, K.; Karvembu, R.; Kim, I. S. Catalytic N-oxidation of tertiary amines on RuO<sub>2</sub> NPs anchored graphene nanoplatelets. *Catal. Sci. Technol.* **2014**, *4*, 2099–2106.

(50) Della Pina, C.; Falletta, E.; Rossi, M. Effect of gold addition on Pt and Pd catalysts in liquid phase oxidations. *Top. Catal.* **2007**, *44*, 319–324.

(51) Prasad, M. R.; Kamalakar, G.; Madhavi, G.; Kulkarni, S. J.; Raghavan, K. V. An efficient synthesis of heterocyclic N-oxides over molecular sieve catalysts. *J. Mol. Catal. A: Chem.* **2002**, *186*, 109–120.

(52) Wabnitz, T.C.; Yu, J. Q.; Spencer, J. B. Evidence that protons can be the active catalysts in lewis acid mediated hetero-Michael addition reactions. *Chem. - Eur. J.* **2004**, *10*, 484–493.

(53) Hayashi, Y.; Rohde, J. J.; Corey, E. J. A novel chiral super-Lewis acidic catalyst for enantioselective synthesis. *J. Am. Chem. Soc.* **1996**, *118*, 5502–5503.

(54) Kantam, M. L.; Laha, S.; Yadav, J.; Jha, S. Nanocrystalline copper (II) oxide catalyzed *aza*-Michael reaction and insertion of  $\alpha$ -diazo compounds into N–H bonds of amines. *Tetrahedron Lett.* **2009**, *50*, 4467–4469.

(55) Tjoa, V.; Jun, W.; Dravid, V.; Mhaisalkar, S.; Mathews, N. Hybrid graphene–metal nanoparticle systems: electronic properties and gas interaction. *J. Mater. Chem.* **2011**, *21*, 15593–15599.

(56) Chen, H.; Muller, M. B.; Gilmore, K. J.; Wallace, G. G.; Li, D. Mechanically strong, electrically conductive, and biocompatible graphene paper. *Adv. Mater.* **2008**, *20*, 3557–3561.

(57) Chang, G.; Bao, Z.; Ren, Q.; Deng, S.; Zhang, Z.; Su, B.; Yang, Y. Fabrication of cuprous nanoparticles in MIL-101: an efficient adsorbent for the separation of olefin–paraffin mixtures. *RSC Adv.* **2014**, *4*, 20230–20233.